Final version of L&O article number 09-366 (pre-proofs)

Published July 2010 Limnology & Oceanography 55(4), 1601-1613

Coccolithophore dynamics in non-bloom conditions during late summer in the central Iceland Basin (July-August 2007)

Alex J. Poulton,[a,*] Anastasia Charalampopoulou,[a] Jeremy R. Young,[b] Glen A. Tarran,[c] Mike I. Lucas,[d] Graham D. Quartly [a].

[a] National Oceanography Centre Southampton, University of Southampton, United Kingdom.

[b] Department of Palaeontology, Natural History Museum, London, United Kingdom.

[c] Plymouth Marine Laboratory, Prospect Place, Plymouth, United Kingdom.

[d] Zoology Department, University of Cape Town, Rondebosch, Cape Town, South Africa.

Corresponding author: aljp@noc.soton.ac.uk

Running head: Iceland Basin coccolithophore dynamics

Acknowledgements

We thank R. Pidcock for assistance with interpreting the physical field, and acknowledge M. Nielsdóttir (iron), M. Stinchcombe (macronutrients), M. Moore (chlorophyll), and A. Martin (physics) for data access. We are grateful to the National Aeronautics and Space Administration (NASA) Goddard Space Flight Center (GSFC) for the routine production of both chlorophyll and calcite products from the Moderate Resolution Imaging Spectroradiometer (MODIS) sensor. We thank the officers and crew of the RRS *Discovery*, the technical staff from the National Marine Facilities, and J. Allen as Principal Scientific Officer for the Biophysical interactions in the Iceland Basin (BIB) cruise. Finally, we would like to thank P. Holligan and two anonymous reviewers for comments on a previous draft of the manuscript. Participation of AJP in the Iceland Basin cruise was supported by Oceans 2025 funding, with further financial support from the Natural Environmental Research Council via a postdoctoral fellowship (NE/F015054/1).

Abstract

Measurements of primary production (PP), calcification (CF), and coccolithophore abundance were made during late summer (July-August 2007) in the Iceland Basin. Low numbers of coccolithophore cells and detached coccoliths (<1 x 10^3 cells mL^{-1} and 1-15 x 10^3 coccoliths mL^{-1}, respectively) indicated a non-bloom community, with *Emiliania huxleyi* as the dominant coccolithophore in terms of abundance, coccolithophore organic biomass, and cell calcite. PP ranged from 0.1-2 mmol C m^{-3}, while CF ranged from 10-250 μmol C m^{-3}, with both typically decreasing with depth. Coccolithophores were estimated to contribute 10-20% towards total chlorophyll *a*, phytoplankton carbon, and PP within the euphotic zone. In these non-bloom conditions, ~30-60% of the total calcite in the water column was present as detached coccoliths rather than whole cells. Both cell numbers and variability in cell-normalised CF controlled the magnitude of total CF, and hence both physiological limits to cell CF and growth, as well as mortality factors, need to be taken into account when examining oceanic coccolithophore communities. Combining cell-normalised CF with an estimate of coccolith calcite gave coccolith production rates (0.4-1.8 h^{-1}) similar to those reported in the literature for laboratory cultures of *E. huxleyi*. None of the factors currently associated with coccolithophore blooms (irradiance, mixed layer depth, nitrate, phosphate, or calcite saturation) showed a clear correlation with community or cellular CF. Hence, although mortality is likely to control cell numbers, other factors such as trace metal (iron) availability may influence coccolithophore physiology in the central Iceland Basin during late summer.

Introduction

Late summer satellite images from high-latitude temperate seas, such as the Iceland Basin and Patagonian Shelf, often show large-scale patches of highly reflective water (Brown and Yoder 1994). These striking features are coccolithophore blooms (Holligan et al. 1993), often dominated by *Emiliania huxleyi*, although other species (e.g., *Coccolithus pelagicus*, *Gephyrocapsa* spp.) are usually present at low relative densities (Malin et al. 1993). The high reflective index of these blooms is caused by the shedding of coccoliths (Holligan et al. 1983; Balch et al. 1999); calcite plates which coccolithophores use to form a composite exoskeleton, the coccosphere. Coccoliths are detached from the coccosphere by both healthy and environmentally stressed cells, with detachment rates low during steady state growth and increasing sharply under nutrient stress (Balch et al. 1993, 1996). In the case of coccolithophore blooms, the white waters detected by satellites are caused by detached coccoliths rather than by cells (Balch et al. 1999), when nutrient concentrations are depleted, rates of primary production (PP) and calcification (CF) are unbalanced, and the coccolithophore community is in decline (Fernández et al. 1993; Holligan et al. 1993).

The factors favoring the formation of coccolithophore blooms, defined as large patches of high reflectance water in satellite images, are considered to be well known, and include high irradiance (photosynthetically active radiation, PAR), shallow mixed layers, high temperatures, and reduced (micro-) zooplankton grazing (Tyrrell and Merico 2004; Raitsos et al. 2006). Phosphate limitation (nitrate: phosphate >16) was originally included as a critical factor (Tyrrell and Merico 2004) based on *E. huxleyi* showing a high affinity for phosphate (Riegman et al. 2000). However, the role of phosphate limitation has now been questioned, as *E. huxleyi* blooms are also found in nitrate limited waters (Lessard et al. 2005). The factors which actually regulate in situ

rates of CF are less well known, both in bloom and non-bloom conditions (Brand 1994; Balch 2004), which is in part due to a limited number of direct measurements.

Coccolithophore cell numbers and community composition have been relatively well studied in the global ocean (Beaufort et al. 2008; Boeckel and Baumann 2008). Such studies of extant coccolithophore communities include comparison of cell numbers with environmental parameters in order to elucidate the factors which control the distribution and growth of coccolithophores. However, this procedure can lead to conflicting results as cell numbers are regulated by growth *and* mortality (grazing, viral lysis: Holligan et al. 1993; Balch 2004; Tyrrell and Merico 2004). Regression of growth factors with community CF (i.e., total-CF) also has inherent problems (Lipsen et al. 2007): culture studies have documented considerable cellular variability in the rate of CF with growth conditions and between species (Paasche 2002). An alternative is to examine the cellular level of CF in the form of cell-specific CF rates (cell-CF), which are proportional to rates of coccolith production when normalized to coccolith calcite, and to compare these with environmental factors. Such cell-specific CF rates can only be considered in terms of coccolith production rates if the community is dominated by a few species, as there is considerable interspecies variability in coccolith calcite (Young and Ziveri 2001). However, few studies exist which have taken this approach (Fernandez et al. 1993; Balch et al. 2000), and hence there is a lack of understanding of the variability in cell-CF in field conditions.

The major goal of this study was to collect measurements of cell-CF from the central Iceland Basin, an important biome for oceanic CF (Holligan et al. 1993). A second goal of this study was to make a comparison of cell-CF with environmental conditions and begin to elucidate what factors control both cellular CF and pelagic

calcite production: a priori, are the factors involved the same as those favoring the formation of coccolithophore blooms? The final goal of this study was to assess the dynamics of the coccolithophore community in the central Iceland Basin, in terms of its production, composition, and contribution to the total phytoplankton community. Sampling was carried out as part of the '*Biophysical interactions in the Iceland Basin (BIB)*' cruise (Fig. 1; Allen and Painter 2008). The timing and location of the BIB cruise (23 July - 24 August 2007) was such that the majority of algal biomass was in coastal waters to the north and along the Reykjanes Ridge to the west (Fig. 1A), the June-July coccolithophore bloom as observed in previous years (Raitsos et al. 2006) had declined (Fig. 1B), the diatom community was limited by both silicate (Brown et al. 2003) and iron (Nielsdöttir et al. 2009), and the majority (60-80%) of algal biomass was in cells <5 μm in diameter (Nielsdöttir et al. 2009). Hence, our measurements were collected during a time when the coccolithophore community was not in a bloom state and the coccolithophore dynamics in non-bloom temperate conditions could be uniquely addressed. As such, this is only the second study to have observed coccolithophore dynamics in the Iceland Basin (Fernandez et al. 1993) or in non-bloom conditions in temperate waters (Lipsen et al. 2007).

Methods

Sampling - The BIB cruise repeatedly sampled a 90 x 90 km grid during late summer in the central Iceland Basin (Fig. 1) for physical, chemical and biological parameters using a combination of Conductivity Temperature Density (CTD) profiles and towed instrumentation (Allen and Painter 2008).Water samples for rate measurements (PP, CF), community structure, and ancillary parameters (chlorophyll *a* (Chl *a*), calcite, and macronutrients) were collected from 11 pre-dawn (02:00-04:00 h

Greenwich Mean Time) deployments of a Seabird 911+ CTD and 24-bottle rosette sampler (Fig. 1). Vertical sampling concentrated on six light depths (55%, 33%, 14%, 7%, 4.5%, and 1% of incident PAR) over the upper water column (0-50 m). The light levels were determined at the start of the cruise, from a calculation of the vertical attenuation coefficient from a daytime CTD cast (Sta. 16202 = 0.098 m^{-1}), and these depths (5, 10, 20, 27, 32, and 47 m) were used throughout the cruise. Post-cruise recalculation of the light depths, using vertical attenuation coefficients from all daytime CTD casts (mean value 0.090 ± 0.015 m^{-1}; n = 20), gave average light depths of 64%, 41%, 16.5%, 8.8%, 5.6%, and 1.5%. Hence, our sampling depths were slightly shallower than the targeted light depths. The depth of 1% incident irradiance (47 m) was assumed to equate to the depth of the euphotic zone and all parameters were integrated to this depth. The depth of the upper mixed layer was determined from the density profiles by identifying the first depth where $\Delta\sigma_t$ m^{-1} (= $\Delta\sigma_t$ / ΔZ, where σ_t is density and Z is depth) was >0.05 m^{-1}, and these were visually confirmed from the density profiles (*see* Fig. 2).

Primary production and calcification - Daily rates (dawn-dawn, 24 h) of PP and CF were determined following the methodology of Paasche and Brubak (1994) and Balch et al. (2000). Water samples (150 mL, 3 light replicates, 1 formalin-killed blank) were collected from each of the six light depths, spiked with 0.26-0.41 MBq (70-110 μCi) ^{14}C-labeled sodium bicarbonate (Amersham) and incubated on deck at 03:00-06:00 h GMT. Formalin-killed blanks were prepared by addition of 5-10 mL of 0.2 μm filtered and borax-buffered formaldehyde solution. On deck incubators were chilled with sea surface water and light depths were replicated using a mixture of misty-blue and grey light filters. Light levels in the incubators were checked with a 4π

scalar PAR irradiance sensor (Biophysical Instruments, QSL-2101) and actual light levels (percentage of incidental irradiance) were: 42.8% (for 55% incubator), 28.0% (33%), 10.8% (14%), 7.1% (7%), 4.3% (4.5%), and 0.4% (1%).

Incubations were terminated after 24 h by filtration through polycarbonate filters (25 mm diameter, 0.2 μm pore size), with extensive rinsing with freshly filtered (<0.7 μm), unlabeled seawater to remove any residual ^{14}C-labeled dissolved inorganic carbon. Filters were then placed in 20 mL glass scintillation vials with gas-tight rubber stoppers and plastic center wells (Kontes) containing Glass-Fibre Whatman filters (GFA) soaked with 0.2 mL β-phenylethylamine (Sigma). Phosphoric acid (1 mL, 1%) was injected through the stopper into the bottom of the vial to convert ^{14}C-labeled calcite to $^{14}CO_2$ which was then caught in the β-phenylethylamine soaked GFA filter. After 20-24 h, the center wells with GFA filters were removed and placed in fresh scintillation vials and Hi-Safe liquid scintillation cocktail (Perkin-Elmer) was added to both vials: one containing the polycarbonate filter (non-acid labile production; PP) and one containing the GFA filter (acid-labile production; CF). Activity in both filters was then determined on a TriCarb 2100TR liquid scintillation counter and counts converted to uptake rates using standard PP methodology. Spike activity was checked by removal of 0.1 mL from one of the three triplicates for each sampling depth after spike addition, mixing with 0.1 mL of β-phenylethylamine, addition of Hi-Safe liquid scintillation cocktail and counting on the TriCarb liquid scintillation counter.

Capture efficiency was ~99.9% and was assessed by sub-sampling from the formalin-killed sample directly after spike addition, acidification with 1% phosphoric acid and determination of the activity collected on the Whatman GFA filter relative to the diluted spike activity. The average relative standard deviation (standard deviation

divided by mean x 100) of triplicate measurements was 13% (1-40%) for PP and 21% (1-78%) for CF. The formalin blanks often represent a significant proportion of the CF signal (this study, mean 21%; range 5-73%), especially when rates are low (Poulton et al. 2007) at the base of the euphotic zone. Measurements of CF on relatively small volumes (~150 mL) measure coccolithophore CF rather than CF associated with large and relatively rare pelagic calcifiers (foraminifera, pteropods).

Coccolithophore and coccolith counts - From each depth where seawater was taken to measure CF, a sample was also collected for the determination of (initial) coccolithophore cell numbers, coccolith abundance and species identification. Water samples (0.5 L) were filtered under gentle pressure through nitrocellulose filters (25 mm diameter, 0.45 μm pore size), with a circle of nylon mesh (25 mm diameter, 10 μm pore size) as a backing filter, oven dried for 6-8 h at 30-40^{o}C and stored in Millipore petri-slides. Permanent slides of the filters were then prepared by mounting the filters using low-viscosity Norland Optical Adhesive (No. 74, Technoptics). Enumeration of coccolithophore cells and loose coccoliths was carried out under cross-polarised light (X1000, oil immersion) using either a Zeiss Axioscope or Olympus BH-2 microscope. Either 300 fields of view (FOV) or 300 individual cells (whichever first) were counted per filter, with a minimum of 50 FOV counted when cells were abundant. Cells were identified down to species following Young et al. (2003). Loose coccoliths of *E. huxleyi* were counted from either full FOV or a quarter of a FOV, from either 50 FOV or for 500 coccoliths (whichever first), with a minimum of 5 FOV when coccoliths were abundant. The organic carbon content of the species present were estimated using light microscope measurements of inner coccosphere diameter (Kovala and Larrence 1966). Cellular (coccosphere) calcite

content for the species present, other than *E. huxleyi*, was calculated by combining individual coccolith calcite (Beaufort and Heussner 1999; Young and Ziveri 2000) with the number of coccoliths per coccosphere (Boeckel and Baumann 2008).

Ancillary parameters - Water samples (100-200 mL) for Chl *a* analysis were filtered onto Whatman GFF (0.7 μm pore size) filters and extracted in 10 mL 90% acetone (High Performance Liquid Chromatography grade) for 20-24 h (dark, 4^{o}C). Measurements of Chl *a* fluorescence were analyzed on a Turner Designs TD-700 fluorometer equipped with Welschmeyer (1994) filters and calibrated using a pure Chl *a* standard (Sigma). Measurements of calcite were made on 500 mL seawater samples filtered onto 0.2 μm pore size polycarbonate filters, rinsed with trace ammonium solution (alkaline pH ~ 9-10), extracted in 2% nitric acid and analysed using a Inductively Coupled Plasma - Optical Emission Spectrometer (ICP-OES). Measurements of particulate organic carbon (POC) were made on 1-2 L seawater samples following Poulton et al. (2006). Macronutrient (nitrate, silicate, phosphate) concentrations were determined following the methodology of Sanders et al. (2007) on a Skalar autoanalyser. Precision of nutrient measurements was ± 0.17 mmol N m^{-3} for nitrate, ± 0.03 mmol P m^{-3} for phosphate, and ± 0.07 mmol Si m^{-3} for silicate.

Satellite data on Chl *a* and calcite concentration (Fig. 1) were obtained from the National Aeronautics and Space Administration (NASA) Goddard Space Flight Center (GFSC) ocean color File Transfer Protocol (FTP) site. These were daily and monthly Level 3 gridded composites of data from MODIS, at a spatial resolution of 0.04^{o} in latitude and longitude.

Cell abundances for phytoplankton other than coccolithophores were analysed from each sampling depth within the euphotic zone, through either flow cytometry

(for *Synechococcus*, picoeukaryotes, and nanoeukaryotes) or light microscopy (for diatoms). Samples for flow cytometry were collected in clean 250 mL polycarbonate bottles and analysed using a Becton Dickinson FACSort instrument to characterise cells based on their light scattering and autofluorescence properties (Allen and Painter 2008). Cell abundances from flow cytometer counts were converted to biomass using literature values (Tarran et al. 2001, 2006). Water samples for diatom counts were collected and preserved with acidic Lugol's solution (2% final solution) in 100 mL amber glass bottles. Diatoms were counted in 50 mL subsamples using a SP-95-I inverted microscope (X200; Brunel Microscopes), and cell counts were converted to biomass following Kovala and Larrence (1966).

Results

General oceanography - During the time of sampling, the Iceland Basin was characterized by several mesoscale eddies and jets (Allen and Painter 2008). The BIB survey grid was characterised by a jet (JET) and filament running diagonally west-east from the northwest corner (*see* satellite Chl *a* in Fig. 1C), and a pair of eddies traveling parallel to the jet (Fig. 1D; Allen and Painter 2008). These two eddies, the northern cyclonic (CYC) and southern anti-cyclonic (ANT), traveled from northwest to southeast across the BIB grid during the cruise (Fig. 1D; Allen and Painter 2008). Using real-time satellite images and underway towed instrumentation to determine the relative position of these three features allowed for targeted sampling (Fig. 1C; Sta. JET, CYC, and ANT) during the latter stages of the cruise. The productivity stations (Fig. 1C) were sampled sequentially and up to a week separated stations of a similar position (Table 1). Due to the strong physical gradients present, temporally-separated

stations which were in similar positions may have been in different water masses, and hence changes cannot be viewed as directly successional.

Surface (5 m) water concentrations of nitrate and phosphate were generally 1.8-3.0 mmol N m^{-3} and ~0.2 mmol P m^{-3}, although concentrations >5 mmol N m^{-3} and >0.3 mmol P m^{-3} were associated with the ANT (Table 1). Silicate concentrations were very low (<0.3 mmol Si m^{-3}), although a few stations (JET, ANT) had levels >0.4 mmol Si m^{-3}. Mixed layer depths were 19-45 m, although the majority of stations had mixed layers ~30 m (Table 1; Fig. 2). The mixed layer was always shallower than the depth of the euphotic zone, indicating that light-limitation was unlikely in the mixed layer. Daily incident PAR irradiance showed 4-fold variability (9.0-39.3 mol PAR m^{-2} d^{-1}) during the cruise with no clear temporal trend (Table 1).

Euphotic zone Chl *a* concentrations were 0.25-0.5 mg m^{-3}, with concentrations >0.75 mg m^{-3} in the CYC (Fig. 2). Profiles of Chl *a* were uniform over the mixed layer, and continued or decreased below to the base of the euphotic zone. Integrated Chl *a* ranged from 8.7 to 35.6 mg m^{-2}, with high values in association with the JET and CYC (Table 1). Integrated POC and calcite was highest overall in the CYC, although the ANT, JET, and Sta. 16226 also showed high values (Table 1). The average integrated ratio of calcite to POC was 0.05 (0.02-0.06), although the CYC had a slightly higher value of 0.09.

Primary production and calcification - Discrete PP rates ranged from 0.1-2 mmol C m^{-3} d^{-1} in this study, with maximum rates in surface waters (5-20 m) and decreasing with depth (Fig. 3). The stations with the highest PP (1.5-2 mmol C m^{-3} d^{-1}) were the JET, Sta. 16260, CYC, and ANT. All stations showed a marked decrease in PP below the mixed layer, and minimum rates of PP were always found at the base

of the euphotic zone (Fig. 3). Integrated PP ranged from 9.9 to 65.3 mmol C m^{-2} d^{-1}, with the highest PP associated with the CYC (Table 1).

Both the vertical profiles and integrated values of CF showed very similar patterns to PP (Fig. 3; Table 1). Discrete rates of CF ranged from 10 to 250 μmol C m^{-3} during the cruise, with maximum rates in the upper 20 m and decreasing with depth in an identical manner to PP. The stations with the highest CF (200-250 μm C m^{-2} d^{-1}) were Sta. 16226, JET, Sta. 16260, CYC, and ANT (Fig. 3). Integrated CF ranged from 1.0 to 7.8 mmol C m^{-2} d^{-1} (Table 1), with the highest integrated CF associated with the CYC.

A statistically significant ($p<0.001$; $n = 66$) relationship was found between discrete measurements of PP and CF, with the slope of the relationship indicating a CF:PP ratio of 0.13 (Fig. 4). The CF:PP ratio was generally ~0.10 over the upper water column but varied from <0.05 to >0.20 at the base of the euphotic zone (Fig. 4). Integrated PP and CF gave similar CF:PP ratios to discrete values (Table 1).

Coccolithophore community structure - A limited number of coccolithophore species were observed by light microscopy: *E. huxleyi* (Fig. 5), *Syracosphaera molischii*, *Coccolithus pelagicus*, and *Syracosphaera pulchra*. Images taken using a 1450VP Scanning Electron Microscope (SEM) of individual coccospheres (Fig. 5A) and detached coccoliths (Fig. 5B) indicate that the A morphotype of *E. huxleyi* was dominant (Young et al. 2003), and each coccosphere had an average of 15 coccoliths (range 10-20). This estimate of coccoliths per coccosphere matches well with other field and culture studies (Paasche 2002; Boeckel and Baumann 2008), and represents a single layer of coccoliths in the coccosphere (Balch et al. 1993; Young et al. 2003).

SEM observations also found ~20 species not seen in the light microscope

counts, although at very low (<1%) relative densities in terms of cells and detached coccoliths. These included: *Acanthoica* spp., *Aligosphaera* sp., *Calcidiscus leptoporus* HOL, *Calcciopappus* spp., *Coccolithus pelagicus, C. pelagicus* HOL, *Corisphaera gracilis, Gephyrocapsa ericsonii, G. muellerae, Helladosphaera cornifera, Ophiaster formosus, Palusphaera vandelii, Pappomonas* spp., *Papposphaera* sp., *Picarola margelefii, Rhabdosphaera xiphos, Sphaerocalyptra* sp. HOL, *Syracosphaera anthos, S. bannockii, S. bannockii* HOL, *S. dilatata, S. molischii, S. molischii* HOL, *S. nana, S. nodosa, S. ossa, S. pulchra, S. tumularis* (A. Charalampopoulou unpubl.).

However, at all stations *E. huxleyi* was dominant in terms of cell numbers (~90%; Table 2) and detached coccoliths (A. Charalampopoulou unpubl.). *S. molischii* was the second most abundant coccolithophore species in terms of cell numbers (1-8%). *E. huxleyi* was also the dominant coccolithophore species in terms of cellular organic carbon (66-90%) and cellular (coccosphere) calcite (68-89%) (Table 2).

Within the euphotic zone, coccolithophore cell numbers and detached coccoliths of *E. huxleyi* ranged from 0.10 to 0.87 x 10^3 cells mL^{-1} and from 0.8 to 15 x 10^3 coccoliths mL^{-1}, respectively (Fig. 6). Vertical profiles of cell numbers showed either uniform profiles (e.g., Sta. 16204) or a sharp decline below the mixed layer and at the base of the euphotic zone (e.g., Sta. 16274). No subsurface maxima in cell numbers was found at any of the sampling stations (Fig. 6). High cell numbers (>0.25-0.50 x 10^3 cells mL^{-1}) were observed at Sta. 16226 (upper 20 m), JET, Sta. 16274, and ANT, with highest cell numbers (>0.80 x 10^3 cells mL^{-1}) in the CYC. Vertical profiles of detached *E. huxleyi* coccoliths typically showed similar patterns to cell numbers (Fig. 6), but sub-surface maxima were observed at Sta. 16226, JET, CYC, and ANT. The ratio of *E. huxleyi* detached coccoliths to cell numbers was >10

at Sta. 16226, JET, Sta. 16260, Sta. 16274, CYC, and ANT, and around or less than 10 at the other stations. Highest coccolith densities (>10 x 10^3 coccoliths mL^{-1}) were found in surface waters at Sta. 16274 and CYC, and at the base of the mixed layer in the JET (Fig. 6). Elevated coccolith densities were also found at the base of the mixed layer at Sta. 16226 and ANT.

Cell-specific calcification - Variability in (total) calcification rates between sampling stations may be due to either changes in cell numbers and/or changes in cell-specific calcification. Hence, normalizing total-CF to coccolithophore cell numbers provides cell-CF, and when coccolith calcite is taken into account, it also provides an estimate of relative coccolith production rates. Vertical profiles of cell-CF (Fig. 7) showed similar profiles to total-CF (Fig. 3): high in surface and subsurface waters and decreasing with depth. However, one station (16226; Fig. 7) did show a sub-surface (20-40 m) maximum with values similar to those found in surface waters at other stations (0.75 pmol C $cell^{-1}$ d^{-1}). Generally, cell-CF showed no marked change in relation to the mixed layer, but was always minimal at the base of the euphotic zone (<0.05 pmol C $cell^{-1}$ d^{-1}). The highest cell-CF (0.75 pmol C $cell^{-1}$ d^{-1}) was found at Sta. 16236 and Sta. 16260, at 30 m at Sta. 16226, while the JET had maximal rates ~0.5 pmol C $cell^{-1}$ d^{-1}, and the ANT and CYC had maximal rates of ~0.25 pmol C $cell^{-1}$ d^{-1}.

Discussion

Coccolithophores and other phytoplankton in the central Iceland Basin - In order to fully assess the effect(s) climate change and ocean acidification will have on coccolithophores, their production and ecology in both bloom and non-bloom conditions needs to be better understood. Coccolithophore blooms are a common

occurrence in the Iceland Basin (Brown and Yoder 1994), and are associated with high cell numbers and significant amounts of calcite (Fernández et al. 1993; Holligan et al. 1993). However, during our study high Chl *a* was restricted to an area to the west of the sampling grid (Fig. 1A) and patches of high reflectance were generally absent (Fig. 1B). Coccolithophore cell and coccolith numbers were relatively low (<1 x 10^3 cells mL^{-1} and 1-15 x 10^3 coccoliths mL^{-1}; Fig. 6) compared with those reported in blooms in the Iceland Basin (5-10 x 10^3 cells mL^{-1} and 100-300 x 10^3 coccoliths mL^{-1}; Fernández et al. 1993). However, as in blooms, *E. huxleyi* was dominant in terms of cell numbers, cell (coccosphere) calcite and coccolithophore biomass (Table 2). The ratio of detached *E. huxleyi* coccoliths to cells (~10) for this study was also lower than those reported in blooms (e.g., 20-30, Fernández et al. 1993). Although the ratio of (total-) CF:PP was significantly higher (0.10-0.14; Table 1) than that observed in low latitude assemblages (~0.03-0.05, Poulton et al. 2007), it was still lower than ratios reported in coccolithophore blooms (e.g., 0.14-0.30, Fernández et al. 1993).

Surface (<20 m) rates of total-CF (100-250 μmol C m^{-3} d^{-1}) were two to five times higher than those measured in tropical and subtropical waters (<50 μmol C m^{-3} d^{-1}; Poulton et al. 2006, 2007), similar to late summer measurements collected in the subarctic NE Pacific (Lipsen et al. 2007), but two to six times lower than those reported from coccolithophore blooms (500-1500 μmol C m^{-3} d^{-1}, Poulton et al. 2007). Total calcite concentrations (Table 1) were also similar to those found in other oceanic settings (e.g., 1.1-110.0 mmol C m^{-2}, Poulton et al. 2007), but lower than those found in coccolithophore blooms (e.g., 142-578 mmol C m^{-2}, Fernández et al. 1993). As well as the statistically significant relationship observed between CF and PP (Fig. 4), significant (p<0.001; n = 11) relationships were also found between integrated Chl *a* and PP (r = 0.96), Chl *a* and CF (r = 0.95) and Chl *a* and calcite (r =

0.87). Such strong relationships between Chl *a* and CF, and between Chl *a* and calcite are not found in datasets from (sub-) tropical waters (Poulton et al. 2007). Their occurrence in the Iceland Basin during late summer and in non-bloom conditions indicates: 1) a strong coupling of Chl *a* and CF, with coccolithophores making up a semi-constant proportion of the total phytoplankton community; 2) a strong coupling of CF with both cellular and detrital (detached coccoliths) calcite; and 3) dominance of the coccolithophore community by a single species (i.e., *E. huxleyi*) even in non-bloom conditions.

In order to further appreciate the contribution of coccolithophores to non-bloom biogeochemical dynamics in the central Iceland Basin, we have estimated coccolithophore contributions to integrated Chl *a*, phytoplankton carbon, PP, and total calcite (Table 3). These estimates indicate that coccolithophores accounted for 10-20% of integrated Chl *a*, phytoplankton carbon, and PP during late summer in the central Iceland Basin. Small flagellates formed the majority of phytoplankton community biomass (Table 3), with only small contributions from *Synechococcus* and diatoms, and the <5 μm fraction accounted for 60-80% of total Chl *a* (Nielsdöttir et al. 2009). Estimates of the amount of integrated calcite associated with coccolithophore cells (coccosphere calcite) varied between 44-72% (Table 3), indicating that ~30-60% of total calcite was present as detached coccoliths (detrital). During the 1991 coccolithophore bloom in the Iceland Basin, ~60-70% of total calcite was as detached coccoliths (Holligan et al. 1993). Hence, even in non-bloom conditions in the central Iceland Basin, ~half to a third of the total calcite in the water column is present as loose coccoliths rather than coccolithophore cells.

Cellular calcification - Variability between sampling stations in terms of total-CF (Fig. 3) were driven by differences in cell numbers (Fig. 6) and/or cell-CF (Fig. 7). For example, although Sta. 16236 and Sta. 16260 were in relatively similar positions (Fig. 1D), they had very different levels of total-CF (Table 1) but almost identical profiles of cell-CF (Fig. 7): variability in total-CF was driven by a doubling of cell numbers (Fig. 6) in the 5-day period between sampling. Conversely, Sta. 16204 and Sta. 16212 had very similar cell numbers (Fig. 6), but different rates of total-CF (Fig. 3): differences at these stations were driven by variability in cell-CF (Fig. 7).

Within this study, sub-surface (<20 m) cell-CF ranged from 0.25-0.75 pmol C $cell^{-1}$ d^{-1}, which is remarkably similar to estimates of cell-CF in *E. huxleyi* cultures (e.g., 0.2-0.8 pmol C $cell^{-1}$ d^{-1}, Balch et al. 1996) and other field studies (e.g., 0.72 pmol C $cell^{-1}$ d^{-1}, Fernández et al. 1993). Regression of detached *E. huxleyi* coccoliths plus coccosphere coccoliths (all species) with discrete measurements of calcite gave a statistically significant relationship (r = 0.78; n = 60; p<0.001), with the slope indicating a carbon content for each coccolith of 0.033 pmol C. This value is similar to estimates from other field studies (e.g., 0.038-0.042 pmol C $coccolith^{-1}$, Holligan et al. 1983; 0.039-0.088 pmol C $coccolith^{-1}$, Fernández et al. 1993), and to values calculated from detailed measurements of *E. huxleyi* coccoliths (0.023-0.048 pmol C $coccolith^{-1}$, Young and Ziveri 2000). Using this estimate of coccolith calcite (0.033 pmol C), the cell-CF values are equivalent to coccolith production rates of between 7-29 coccoliths d^{-1} or 0.4-1.8 coccoliths h^{-1} over a 16 h light period. These values are also similar to those found in *E. huxleyi* cultures (e.g., 0-3 coccoliths h^{-1}, Balch et al. 1996) and field studies (e.g., 0.3-0.5 coccoliths h^{-1}, Fernández et al. 1993). Slight differences between our estimates of coccolith production rates and those of Fernandez et al. (1993) are likely to be due to differences in the estimated coccolith

calcite for the two studies (0.033 pmol C coccolith^{-1} from this study; 0.039-0.088 pmol C coccolith^{-1} from Fernandez et al. 1993).

High coccolith production rates relative to those reported from laboratory cultures imply efficient cellular CF in the central Iceland Basin during non-bloom late summer conditions. Although under severe nutrient (nitrate, phosphate) or light stress, cellular photosynthesis and CF become decoupled (Balch et al. 1996; Paasche 2002), leading to sub-optimal growth rates (Müller et al. 2008), during steady-state growth (Fritz and Balch 1996) and iron stress (Schultz et al. 2004) the two processes appear to remain closely linked. During the onset of nutrient and light stress, coccoliths are detached as layers (Balch et al. 1993), whereas during steady-state growth, coccolith detachment rates are correlated with the growth rate, and of the order of ~1-2 coccoliths cell^{-1} d^{-1} (Fritz and Balch 1996).

Assuming steady state balanced growth for the central Iceland Basin coccolithophore community, combining cell calcite with cell-CF gives an estimate of coccolithophore growth rates (herein μ = 1/cell calcite x cell-CF). These estimated growth rates range from 0.2 to 0.9 d^{-1} (Table 3), with the highest rates (>0.8 d^{-1}) at Sta. 16226, 16236, and 16260. These estimated growth rates are based on initial cell numbers, and therefore represent gross growth rates, unadjusted for losses through mortality. If we were to include steady-state coccolith detachment rates, the rates would only decrease by ~10%. The relatively low ratio of detached coccoliths to cells found in this study (~10; Fig. 6) also supports our assumption of minimal coccolith detachment rates. Although elevated ratios of detached coccoliths to cells were observed at a few stations (e.g., JET), due to the slow sinking speed of individual coccoliths (<0.01 m d^{-1}) it is unclear what proportion of the detached coccoliths

present in the water column are artifacts left over from the earlier bloom and/or advected from outside the study area.

By combining phytoplankton carbon with rates of PP, we can also estimate the growth rate of the total phytoplankton community (Table 3). Coccolithophore and total phytoplankton growth rates estimated in this way compare well, and indicate that both components are growing at similar rates. The phytoplankton community during late summer in the central Iceland Basin was mainly composed of small picoplankton and naked flagellates (Table 3), and hence the close match between the growth rates of coccolithophores and the total phytoplankton community also supports our estimated coccolithophore growth rates. Further, if we compare our estimates of coccolithophore growth rates (μ) with maximum values (μ_{max}) reported for *E. huxleyi* cultures growing in optimum temperature, light and nutrient conditions (1.6 d^{-1}; Paasche 2002), we get an average growth efficiency (μ/μ_{max} x 100) for the central Iceland Basin coccolithophore community of ~33% (range 15-54%).

Environmental controls on cell-CF may include irradiance, macronutrient concentrations, calcite saturation state and trace metal availability, in part due to the strong physiological relationship between cellular CF and photosynthesis (Brand 1994; Paasche 2002). Evidence for a relationship between irradiance and CF can be seen from the trend for both total-CF (Fig. 3) and cell-CF to decrease with depth (Fig. 7), and if cell-CF is plotted against incubation irradiance a hyperbolic curve resembling a photosynthesis vs. irradiance (P vs. E) relationship is observed (A. Poulton unpubl.; Fernández et al. 1993). Low ratios of CF:PP at depth may be due to the greater influence of light on rates of photosynthesis (PP) than on CF (Balch et al. 1996). However, no relationship was found between maximum values of cell-CF, as observed in surface (5 m) waters, and incident irradiance (Fig. 8A). Hence, although

irradiance may have a strong control over the vertical variability of cell-CF, other factors are more important for mesoscale variability. Mixed layer depth, nitrate concentration, phosphate concentration, and the ratio of nitrate to phosphate, all showed no obvious relationship to cell-CF (Fig. 8B-E).

Calculations of calcite saturation ($\Omega_{calcite}$) from dissolved inorganic carbon and alkalinity measurements during the BIB cruise showed little variability between sampling stations (range 4.4-4.9), and no clear relationship was observed between $\Omega_{calcite}$ and surface CF-cell (A. Charalampopoulou unpubl.). Nielsdóttir et al. (2009) made concurrent measurements of dissolved iron during the BIB cruise and found extremely low iron concentrations (average 0.091 ± 0.098 nmol L^{-1}), as well as very low iron to nitrate ratios (<0.02 mmol:mol), both of which are likely to be growth limiting for phytoplankton (Sunda and Huntsman 1995). Concurrent iron enrichment experiments during the BIB cruise observed a strong response by the phytoplankton community to iron addition, and a dramatic increase in cell numbers of *E. huxleyi* (Nielsdóttir et al. 2009). Unfortunately, CF and coccolith counts were not conducted as part of the study by Nielsdóttir et al. (2009), and no direct examination can be made between cell-CF and iron. Unlike limitation by nitrate, phosphate or irradiance, which all cause decoupling between cellular photosynthesis and CF (Müller et al. 2008), iron limitation appears to lead to concurrent decreases in both photosynthesis and CF (Schultz et al. 2004), and hence lowered growth rates.

Non-bloom coccolithophore dynamics in the central Iceland Basin - To summarize, this study sampled an *E. huxleyi* dominated coccolithophore community in the central Iceland Basin during late summer and in non-bloom conditions. Our observations indicate that in non-bloom conditions in the central Iceland Basin: 1)

coccolithophores may account for 10-20% of the total phytoplankton community's biomass and production; 2) detached coccoliths may account for ~half to a third of the total calcite standing stock; 3) both cell-CF and cell numbers control the magnitude of total-CF, and mesoscale variability in both affects spatial variability in total-CF; 4) the coccolithophore community was producing ~0.4-1.8 coccoliths h^{-1}, which is of the same magnitude as found in mono-specific laboratory cultures of *E. huxleyi* (Balch et al. 1996), and in another field study in the Iceland Basin during a bloom (Fernandez et al. 1993); 5) the coccolithophore community appeared to be growing at a similar rate (0.2-0.9 d^{-1}) to the total phytoplankton community (0.3-0.6 d^{-1}), and with a growth efficiency of ~30%; and 6) total-CF and cell-CF showed no clear correlation with any of the factors currently associated with coccolithophore blooms (i.e., irradiance, mixed layer depth, phosphate limitation). However, independent iron enrichment experiments (Nielsdóttir et al. 2009) indicate that iron availability may exert a strong control on cell-CF and total-CF.

Overall, it appears that even in non-bloom conditions, coccolithophores make a significant contribution to biogeochemical cycles in the central Iceland Basin, and CF rates in non-bloom temperate waters may be two to five times higher than those found in (sub-)tropical waters (Poulton et al. 2007). In the context of future ocean acidification research, our observations highlight the need to combine information on coccolithophore diversity with calcification rates in order to examine trends in cellular calcification, and to also account for the other environmental (e.g., trace metal availability) and ecological (e.g., mortality) factors influencing the coccolithophore community.

References

Allen, J. T., and S. C. Painter. 2008. RRS *Discovery* Cruise 321, 24 July-23 August 2007: Biophysical interactions in the Iceland Basin. National Oceanography Centre, Southampton, Cruise Report No.23, Available at http://eprints.soton.ac.uk/50095

Balch, W. M., K. A. Kilpatrick, P. M. Holligan, and T. L. Cucci. 1993. Coccolith production and detachment by *Emiliania huxleyi* (Prymnesiophyceae). J. Phycol. **29**: 566-575.

Balch, W. M., J. J. Fritz, and E. Fernández. 1996. Decoupling of calcification and photosynthesis in the coccolithophore *Emiliania huxleyi* under steady-state light-limited growth. Mar. Ecol. Prog. Ser. **142**: 87-97.

Balch, W. M., D. T. Drapeau, T. L. Cucci, R. D. Vaillancourt, K. A. Kilpatrick, and J. J. Fritz. 1999. Optical backscattering by calcifying algae: Separating the contribution by particulate inorganic and organic carbon fractions. J. Geophys. Res. **104:** 1451-1558.

Balch, W. M., D. T. Drapeau, and J. J. Fritz. 2000. Monsoonal forcing of calcification in the Arabian Sea. Deep Sea Res. II **47**: 1301-1337.

Balch, W. M. 2004. Re-evaluation of the physiological ecology of coccolithophores, p. 165-190. *In* H. R. Thierstein and J. R. Young [eds.], Coccolithophores from molecular processes to global impact. Springer.

Beaufort, L., and S. Heussner. 1999. Coccolithophorids on the continental slope of the Bay of Biscay - production, transport and contribution to mass fluxes. Deep Sea Res. II **46:** 2147-2174.

Beaufort, L., M. Couapel, N. Buchet, H. Claustre, and C. Goyet. 2008. Calcite production by coccolithophores in the south east Pacific Ocean. Biogeosci. **5**: 1101-1117.

Boeckel, B., and K. H. Baumann. 2008. Vertical and lateral variations in coccolithophore community structure across the subtropical frontal zone in the South Atlantic Ocean. Mar. Micropalaeo. **67:** 255-273.

Brand, L. E. 1994. Physiological ecology of marine coccolithophores, p. 39-50. *In* A. Winter and W. G. Siesser [eds.], Coccolithophores. Cambridge University Press.

Brown, C. W., and J. A. Yoder. 1994. Coccolithophorid blooms in the global ocean. J. Geophys. Res. **99**: 7467-7482.

Brown, L., R. Sanders, G. Savidge, and C. H. Lucas. 2003. The uptake of silica during the spring bloom in the Northeast Atlantic Ocean. Limnol. Oceanogr. **48**: 1831-1845.

Fernández, E., P. Boyd, P. M. Holligan, and D. S. Harbour. 1993. Production of organic and inorganic carbon within a large-scale coccolithophore bloom in the northeast Atlantic Ocean. Mar. Ecol. Prog. Ser. **97**: 271-285.

Fritz, J. J., and W. M. Balch. 1996. A coccolith detachment rate determined from chemostat cultures of the coccolithophore *Emiliania huxleyi*. J. Exp. Mar. Biol. Ecol. **207**: 127-147.

Holligan, P. M., M. Viollier, D. S. Harbour, P. Camus, and M. Champagne-Philippe. 1983. Satellite and ship studies of coccolithophore production along a continental shelf edge. Nature **304**: 339-342.

Holligan, P. M., E. Fernández, J. Aiken, W. M. Balch, P. Boyd, P. H. Burkhill, M. Finch, S. B. Groom, G. Malin, K. Muller, D. A. Purdie, C. Robinson, C. C. Trees, S. M. Turner, and P. van der Wal. 1993. A biogeochemical study of the

coccolithophore, *Emiliania-huxleyi*, in the North Atlantic. Glob. Biogeochem. Cycles **7**: 879-900.

Kovala, P. E., and J. D. Larrence. 1966. Computation of phytoplankton number, cell volume, cell surface and plasma volume per litre, from microscopical counts. Department of Oceanography, University of Washington, Spec. Rep. No. 38.

Lessard, E. J., A. Merico, and T. Tyrrell. 2005. Nitrate:phosphate ratios and *Emiliania huxleyi* blooms. Limnol. Oceanogr. **50**: 1020-1024.

Lipsen, M. S., D. W. Crawford, J. Gower, and P. J. Harrison. 2007. Spatial and temporal variability in coccolithophore abundance and production of PIC and POC in the NE subarctic Pacific during El Nino (1998), La Nina (1999) and 2000. Prog. Oceanogr. **75**: 304-325, doi:10.1016/j.pocean.2007.08.004

Malin, G., S. Turner, P. Liss, P. Holligan, and D. Harbour. 1993. Dimethylsulphide and dimethylsulphoniopropionate in the Northeast Atlantic during the summer coccolithophore bloom. Deep Sea Res. I **40**:, 1487-1508.

Müller, M., A. Antia, and J. LaRoche. 2008. Influence of cell cycle phase on calcification in the coccolithophore *Emiliania huxleyi*. Limnol. Oceanogr. **53**: 506-512.

Nielsdóttir, M. C., C. M. Moore, R. Sanders, D. J. Hinz, and E. P. Achterberg. 2009. Iron limitation of the postbloom phytoplankton communities in the Iceland Basin. Global Biogeochem. Cycles **23**: GB3001, doi:10.1029/2008GB003410

Paasche, E., and S. Brubak. 1994. Enhanced calcification in the coccolithophorid *Emiliania huxleyi* (Haptophyceae) under phosphorus limitation. Phycol. **33**: 324-330.

Paasche, E. 2002. A review of the coccolithophorid *Emiliana huxley*i (Prymnesiophyceae), with particular reference to growth, coccolith formation and calcification-photosynthesis interactions. Phycol. **40**: 503-529.

Poulton, A. J., R. Sanders, P. M. Holligan, M. C. Stinchcombe, T. R. Adey, L. Brown, and K. Chamberlain. 2006. Phytoplankton mineralisation in the tropical and subtropical Atlantic Ocean. Global Biogeochem. Cycles **20**: GB4002, doi:10.1029/2006GB002712

Poulton, A. J., T. R. Adey, W. M. Balch, and P. M. Holligan, 2007. Relating coccolithophore calcification rates to phytoplankton community dynamics; regional differences and implications for carbon export. Deep-Sea Res. II **54**: 538-557, doi:10.1016/j.dsr2.2006.12.003

Raitsos, DE., S. J. Lavender, Y. Pradhan, T. Tyrell, P. C. Reid, and M. Edwards. 2006. Coccolithophore bloom size variation in response to the regional environment of the subarctic North Atlantic. Limnol. Oceanogr. **51**: 2122-2130.

Riegman, R., W. Stolte, A. A. M. Noordeloos, and D. Slezak. 2000. Nutrient uptake and alkaline phosphatase (EC 3:1:3:1) activity of *Emiliania huxleyi* (Prymnesiophyceae) during growth under N and P limitation in continuous cultures. J. Phycol. **36**: 87-96.

Sanders, R., P. J. Morris, M. C. Stinchcombe, S. Seeyave, H. Venables, and M. I. Lucas. 2007. New production and the *f* ratio around the Crozet Plateau in austral summer 2004-2005 diagnosed from seasonal changes in inorganic nutrient levels. Deep Sea Res. II **54**: 2191-2207.

Schultz, K. G., I. Zondervan, L. J. A. Gerringa, K. R. Timmermans, M. J. W. Veldhuis, and U. Riebesell. 2004. Effect of trace metal availability on coccolithophorid calcification. Nature **430**: 673-676.

Sunda, W. G., and S. A. Huntsman. 1995. Iron uptake and growth limitation in oceanic and coastal phytoplankton. Mar. Chem. **50**: 189-206.

Tarran, G. A., M. V. Zubkov, M. V. Sleigh, P. H. Burkill, and M. Yallop. 2001. Microbial community structure and standing stocks in the NE Atlantic in June and July of 1996. Deep Sea Res. II **48**: 963-985.

Tarran, G. A., J. L. Heywood, and M. V. Zubkov. 2006. Latitudinal changes in the standing stocks of nano- and picoeukaryotic phytoplankton in the Atlantic Ocean. Deep Sea Res. II **53**: 1516-1529.

Tyrrell, T., and A. Merico. 2004. *Emiliania huxleyi*: bloom observations and the conditions that induce them, p. 75-90. *In* HR. Thierstein and JR. Young [eds.], Coccolithophores from molecular processes to global impact. Springer.

Welschmeyer, N. A. 1994. Fluorometric analysis of chlorophyll *a* in the presence of chlorophyll *b* and phaeopigments. Limnol. Oceanogr. **39**: 1985-1992.

Young, J. R., and P. Ziveri. 2000. Calculation of coccolith volume and its use in calibration of carbonate flux estimates. Deep Sea Res. II **47**: 1679-1700.

Young, J. R., M. Geisen, L. Cros, A. Kleijne, C. Sprengel, I. Probert, and J. B. Østergaard. 2003. A guide to extant coccolithophore taxonomy. J. Nannoplank. Res. Special Issue **1**: 1-132.

Table 1. Key features of the BIB productivity stations.

Station	Date	Latitude, Longitude	Surface macronutrients (mmol m^{-3})			Mixed layer (m)	Incident irradiance (mol PAR m^{-2} d^{-1})	Euphotic zone (0-47 m) integrals					
			NO_3	PO_4	$Si(OH)_4$			Chl *a* (mg m^{-2})	POC (mmol C m^{-2})	Calcite (mmol C m^{-2})	PP (mmol C m^{-2} d^{-1})	CF (mmol C m^{-2} d^{-1})	CF:PP (mol:mol)
16204	29 July	59.59°N, 19.52°W	1.8	0.20	0.25	43	26.4	10.2	378	13.6	16.9	1.7	0.10
16209	30 July	59.41°N, 20.25°W	2.6	0.18	0.17	31	9.0	12.4	457	14.3	10.9	1.1	0.10
16212	31 July	59.42°N, 18.45°W	2.5	0.18	0.16	33	39.3	12.7	338	6.7	22.8	2.3	0.10
16222	02 Aug	58.51°N, 19.52°W	2.7	0.24	0.16	31	17.0	8.7	329	6.7	9.9	1.0	0.10
16226	05 Aug	58.51°N, 21.00°W	2.3	0.24	0.25	35	26.7	21.0	432	19.9	41.1	5.6	0.14
16236	07 Aug	59.08°N, 19.18°W	2.4	0.25	0.23	33	15.7	16.5	243	5.7	17.7	2.3	0.13
JET	10 Aug	59.59°N, 20.27°W	3.0	0.27	0.51	31	17.5	28.3	431	25.3	48.8	5.5	0.11
16260	12 Aug	59.11°N, 19.05°W	3.2	0.25	0.38	33	19.8	22.9	346	15.8	40.8	4.5	0.11
16274	14 Aug	59.12°N, 19.53°W	5.0	0.33	0.70	19	34.8	20.2	299	13.9	27.7	3.9	0.14
CYC	18 Aug	59.39°N, 18.44°W	2.5	0.18	0.26	45	32.2	35.6	495	42.6	65.3	7.8	0.12
ANT	19 Aug	59.14°N, 19.45°W	5.3	0.32	0.75	29	19.0	23.3	318	17.4	40.4	3.9	0.10
		mean	3.0	0.24	0.35	33	23.4	19.3	370	16.5	31.1	3.6	0.11
		min	1.8	0.18	0.16	19	9.0	8.7	243	5.7	9.9	1.0	0.10
		max	5.3	0.33	0.75	45	39.3	35.6	495	42.6	65.3	7.8	0.14

Table 2. Euphotic zone coccolithophore community composition in terms of standardized cell abundances, organic biomass, and coccosphere calcite from *Emiliania huxleyi* and the rest of the community.

Station	Abundance (%)		Organic biomass (%)		Calcite (%)	
	E. huxleyi	others	*E. huxleyi*	others	*E. huxleyi*	others
16204	98	2	88	12	79	21
16209	98	2	89	11	84	16
16212	95	6	77	23	77	23
16222	98	2	90	10	89	11
16226	97	3	82	18	79	21
16236	96	4	78	22	79	21
JET	93	7	70	30	69	31
16260	94	6	73	27	74	26
16274	96	4	81	19	81	19
CYC	93	7	69	31	71	29
ANT	92	8	66	34	68	32
mean	96	4	79	21	77	23
min	92	2	66	10	68	11
max	98	8	90	34	89	32

Table 3. Coccolithophore contributions to euphotic zone integrals (Chl *a*, phytoplankton carbon, primary production, calcite), a comparison of integrated biomass for the different phytoplankton groups (with coccolithophore contributions to the total in parentheses), and estimates of the growth rates for the coccolithophore and total phytoplankton community.

Station	Coccolithophore contributions (%)				Euphotic zone (0-47 m) integral biomass (mmol C m^{-2})					Growth rates (d^{-1})	
	Chl *a*[1]	Phytoplankton carbon[2]	Primary production[3]	Calcite[4]	SYN[5]	PEUK[5]	NEUK[5]	Diatoms[6]	Coccolithophores	Coccolithophores	Phytoplankton
16204	13	14	14	65	4.8	24.2	161.8	2.1	4.6 (2%)	0.5	0.5
16209	14	14	14	72	2.7	17.4	133.6	3.5	5.8 (4%)	0.2	0.3
16212	10	11	14	60	4.9	16.9	59.7	0.2	4.7 (5%)	0.7	0.5
16222	16	16	14	70	3.3	17.4	84.2	0.8	4.5 (4%)	0.3	0.3
16226	12	12	19	45	9.6	32.5	63.8	0.7	8.7 (8%)	0.9	0.6
16236	7	7	19	62	2.1	9.5	69.8	na	4.1 (5%)	0.8	0.3
JET	12	15	16	44	65.5	36.7	40.7	1.5	14.1 (9%)	0.6	0.5
16260	9	11	16	53	5.4	50.3	143.7	0.6	8.1 (4%)	0.8	0.5
16274	23	24	20	52	na	na	na	0.8	16.4 (na)	0.3	0.4
CYC	22	26	17	59	3.4	67.8	252.3	0.2	30.9 (9%)	0.4	0.6
ANT	19	24	14	53	12.6	40.2	171.8	1.2	18.8 (8%)	0.3	0.5
mean	14	16	16	58	11.4	31.3	118.1	1.2	11.0 (6%)	0.5	0.5
min	7	7	14	44	2.1	9.5	40.7	0.2	4.1 (2%)	0.2	0.3
max	23	26	20	72	65.5	67.8	252.3	3.5	30.9 (9%)	0.9	0.6

[1] From cell numbers and cellular Chl *a* of 0.2 pg (Paasche 2002); [2] From cell biomass and phytoplankton carbon (= Chl *a* x carbon to Chl *a* ratio of 40); [3] Using cell-CF to photosynthesis ratio of 0.7 (Poulton et al. 2006, 2007); [4] From cell numbers and cell calcite values for all species; [5] From flow cytometer derived biomass of *Synechococcus* (SYN), picoeukaryotes (PEUK), and nanoeukaryotes (NEUK) (*see* Methods); [6] Diatom biomass determined from light microscope measurements (*see* Methods).

FIGURE LEGENDS

Fig. 1. Surface Chl *a* and calcite in the Iceland Basin during August 2007. (A) Surface Chl *a* and BIB survey grid (white square). (B) Surface calcite and BIB survey grid (white square). (C) Surface Chl *a* and productivity stations (*see* Table 1). (D) Surface calcite and physical features identified from current data (Allen and Painter 2008) and dynamic height (R. Pidcock pers. comm.). (A-B) Monthly composites of MODIS data. (C-D) Log-averaged composites of daily MODIS data 23 July - 19 August.

Fig. 2. Profiles of Chl *a* and density.

Fig. 3. Profiles of PP and CF.

Fig. 4. Relationship between discrete rates of CF and PP, with model II regression and dashed lines indicating relative ratios.

Fig. 5. (A) SEM image of *Emiliania huxleyi* cells (10 m, Sta. 16285). (B) SEM image of detached *E. huxleyi* coccoliths (10 m, Sta. 16274).

Fig. 6. Profiles of coccolithophore cell numbers and detached *E. huxleyi* coccoliths.

Fig. 7. Profiles of calcification per cell.

Fig. 8. (A) Surface cell-CF and incident irradiance. (B) Surface cell-CF and mixed layer depth. (C) Surface cell-CF and nitrate concentration. (D) Surface cell-CF and phosphate concentration. (E) Surface cell-CF and the ratio of nitrate to phosphate.

Figure 1.

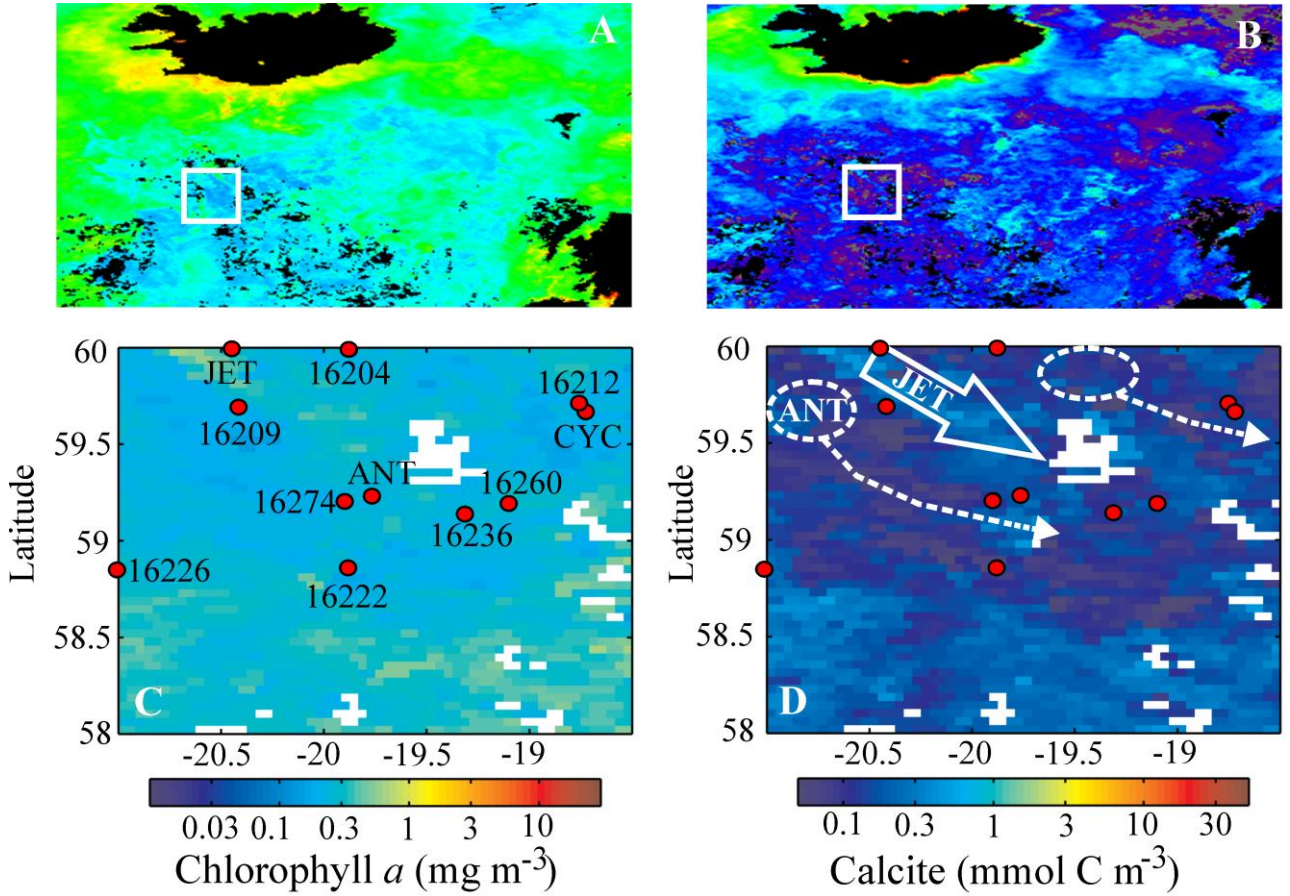
A
B
C
D
JET
16204
16212
16209
CYC
ANT
16260
16274
16236
16226
16222
60
59.5
59
58.5
58
Latitude
-20.5
-20
-19.5
-19
0.03 0.1 0.3 1 3 10
Chlorophyll a (mg m-3)
0.1 0.3 1 3 10 30
Calcite (mmol C m-3)

Poulton et al.

Figure 2.

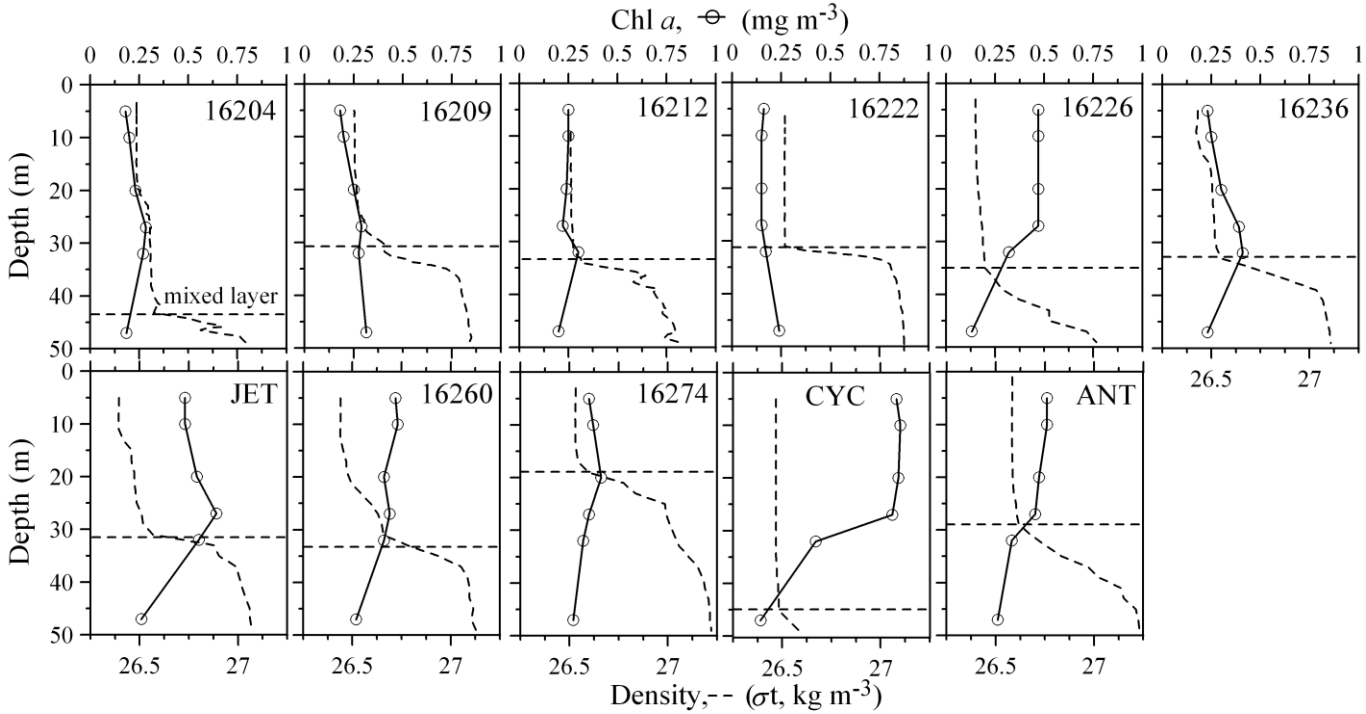

Poulton et al.

Figure 3

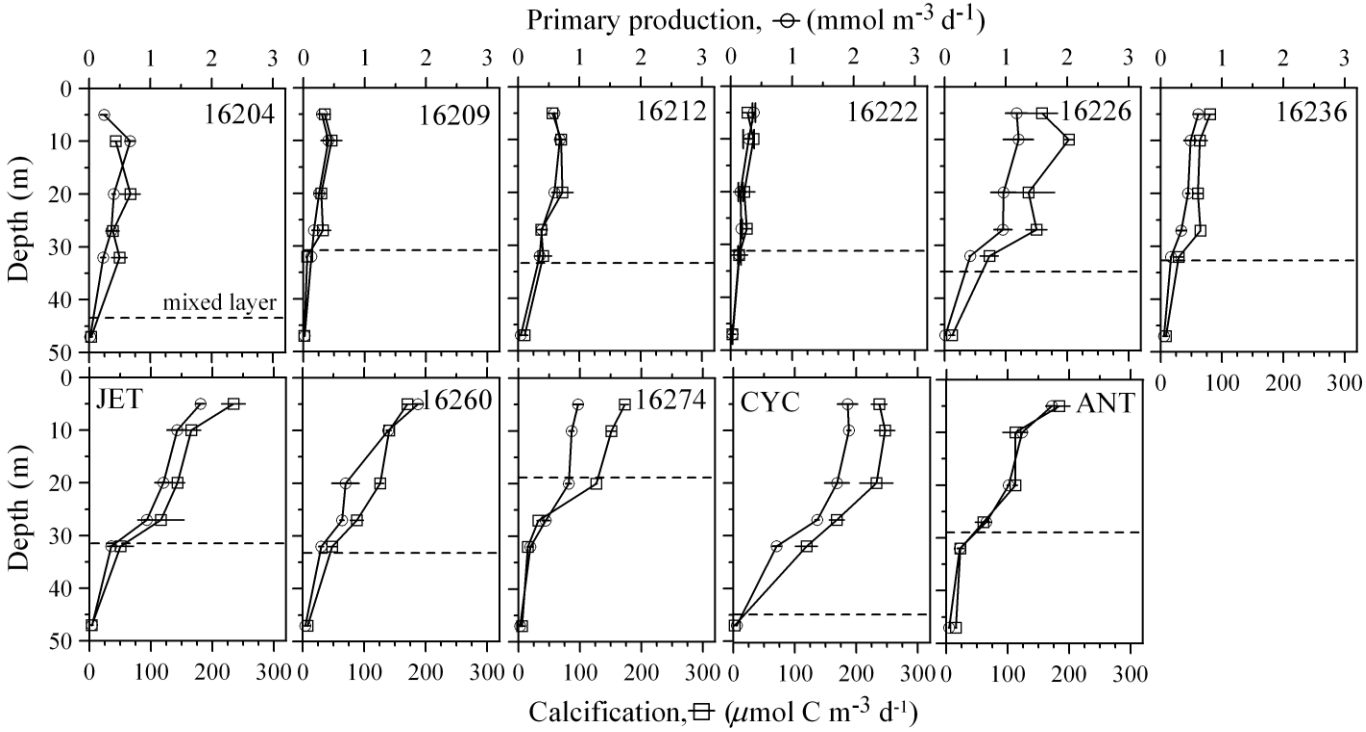

Poulton et al.

Figure 4

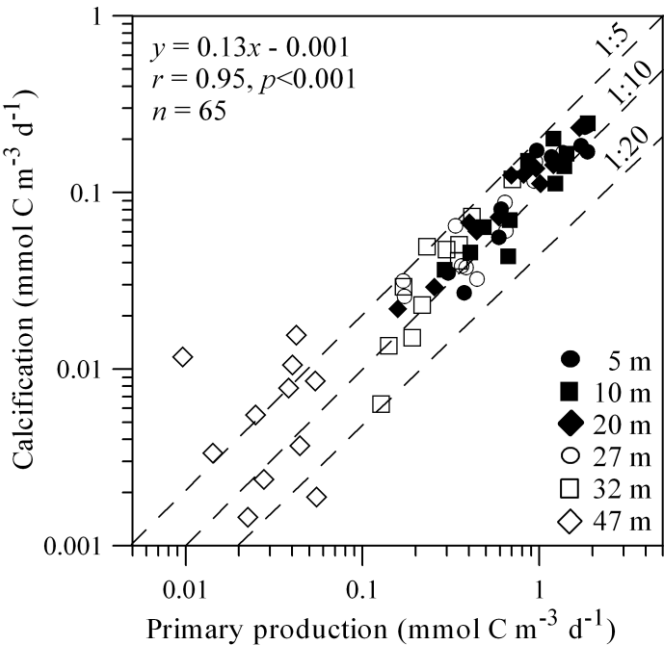

Poulton et al.

Figure 5

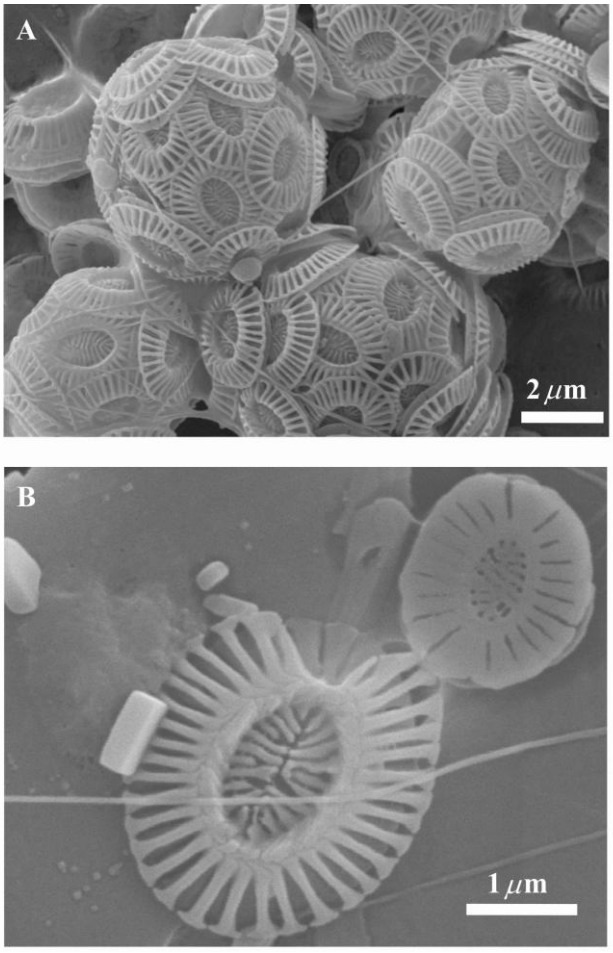

Poulton et al.

Figure 6

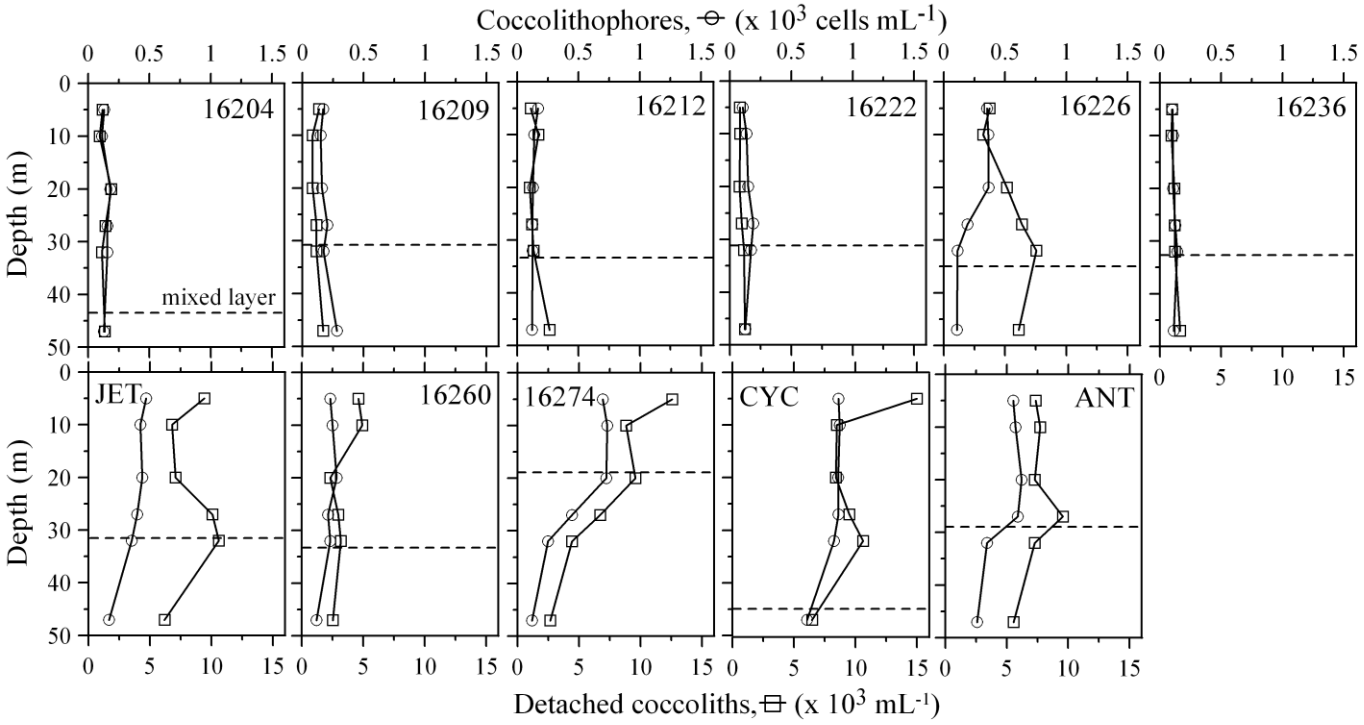

Poulton et al.

Figure 7

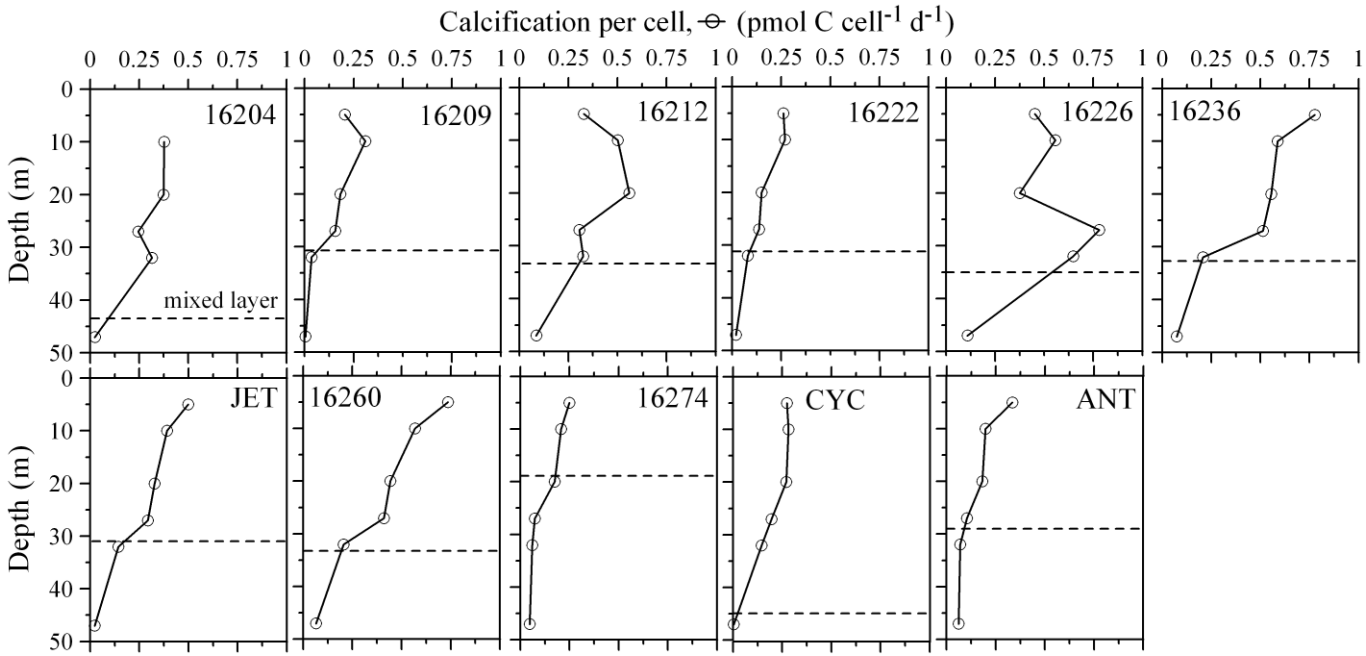

Poulton et al.

Figure 8